4D-Photoluminescence microscope based on Single Pixel Imaging for characterization of semiconductors

Marie Legrand, Adrien Bercegol, Laurent Lombez, Jean-François Guillemoles, Daniel Ory

4D-Photoluminescence microscope based on Single Pixel Imaging for characterization of semiconductors

Marie Legrand * [ab], Adrien Bercegol [ab], Laurent Lombez [ad], Jean-François Guillemoles [bc], Daniel Ory [ab]

[a]EDF R&D, 18bd Thomas Gobert, 91120 Palaiseau France ; [b]Institut Photovoltaïque d'Ile de France (IPVF), 18bd Thomas Gobert, 91120 Palaiseau, France ; [c]CNRS, Ecole Polytechnique, IP Paris, UMR IPVF, France, 18bd Thomas Gobert, 91120 Palaiseau ; [d]Laboratoire de Physique et Chimie des Nano-objets, 135 avenue de Rangueil, 31000 France

ABSTRACT

Analyzing the photoluminescence (PL) maps of semiconductors complementarily in time and wavelength allows to derive their key optoelectronic and transport properties. Up to now, separate acquisitions along time or wavelength had to be acquired for time and wavelength so that a comprehensive study of the dynamics was out of reach. We developed a 4D imaging set-up that allows the simultaneous acquisition of spectral and temporal luminescence intensity with micrometric spatial resolution under the exact same experimental conditions. This novel set-up relies on single pixel imaging, an approach that enables the reconstruction of the spatial information recorded from a higher resolution non-imaging detector. The sample PL signal is spatially modulated with different patterns by a digital micro-mirror device[1]. We make use of this technique for the first time with a streak camera as a detector, allowing to record the PL intensity decays and spectrum for each pixel with very high temporal (<100ps) and spectral resolutions (< 1nm). A patent application has been filled.

We demonstrate the use of this setup by characterizing III-V samples. We observe the spatial variations of a red shift occurring during the short time of the decay.

Keywords: Single Pixel Imaging, Digital Micro-mirror Device, Hyperspectral Imaging, Time resolved imaging

1. INTRODUCTION

The development of innovative photovoltaic materials and architectures benefit from the advancement of characterization methods. In that frame, photoluminescence (PL) measurements, directly related to photovoltaic conversion processes, provides invaluable information to understand the limitations of different structures. As contactless characterization methods, they offer a way to investigate thin films of absorbers as well as the influence of the additional layers[1]. In particular, the obtention of the photoluminescence resolved spectrally allows the extraction of the quasi Fermi levels splitting and therefore probes the potential of the material itself.

The luminescence emitted by the semiconductors depends on a variety of factors. It first requires the generation of carriers by either absorption of light or application of a voltage. These ones thermalize and spread within the material under the influence of drift, diffusion and traps. In competition with luminescence, the non-radiative recombinations can happen (Augers, defects). Consecutively, the emitted photon can be re-absorbed and occasionally contribute to photon recycling. On the one hand, the luminescence spectrum carries the signature of the electronic distribution and photons propagation through the material[2]. On the other hand, capturing the evolution of the luminescence intensity after a pulsed excitation reflects the transport of carriers[3]. Furthermore, imaging these open the door to inhomogeneity studies or experiments under gradient conditions. In this paper, we introduce a novel set-up that provides the local evolution of the PL spectra emitted by a sample. More than providing the simultaneous acquisition of hyperspectral and time-resolved images of photovoltaic material, the 4D data offers a new insight in spectral dynamics.

In fact, the literature provides examples of phenomena leading to spectral changes at short times. Two photons PL experiments have highlighted the dependency of the PL spectrum with the depth of emission[4]. Spectral changes could carry visible signatures of the diffusion in depth and would offer a way to probe the difference with the lateral diffusion

in 2D materials. Moreover, such data can help disentangling optical and electronic transport as it was demonstrated by quantifying photon recycling and band filling impact in perovskites through the induced spectral modifications[5,6].

2. SINGLE PIXEL IMAGING

The 4D-PL set-up is based on Single Pixel Imaging (SPI) technique to reconstruct cartographies from a streak camera coupled to a spectrometer. We describe the concept in this section and give some insight into the necessary noise management to reach the best possible resolution.

2.1 Single Pixel Imaging Concept

Single Pixel Imaging consists in acquiring spatial information from a non-imaging detector. In the same way as raster scanning, it relies on a sequence of measurements that allows encoding temporally the spatial information. As pictured in Figure 1, the sample is characterized by masking different surface areas of the sample. This is achieved by filtering the emitted light through a set of patterns with spatial light modulators. In particular, it can be performed with Digital micro-mirror devices (DMD), which consists in an array of mirrors that can take either a "on" or a "off" position.

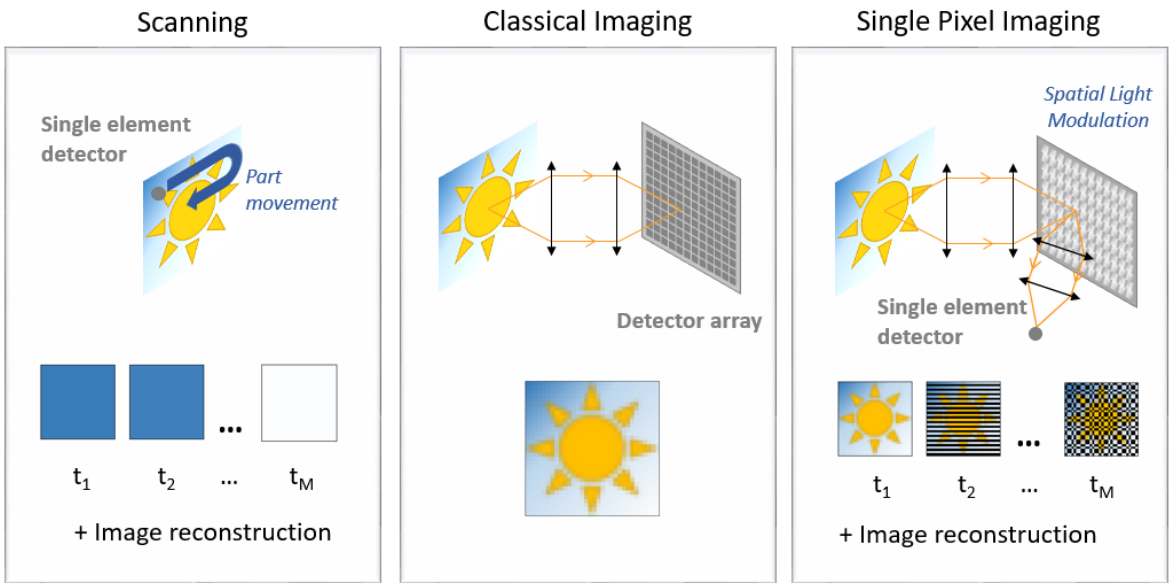

Figure 1: Single Pixel Imaging principle compared with raster scanning and classical imaging

For a given pattern i, the photodetectors captures a signal b_i consisting in the light flux x emitted from the object modulated by the transmission a_i of the set-up. By considering the transmission of the DMD in each of its n mirrors $a_{i,k}$ and $x_{i,k}$ the light flux impinging on it, it the collected light flux is estimated as $b_i = \sum_{k=1}^{n} a_{i,k} * x_k$. This equation can be written for the overall m measurements. Therefore, reconstructing an image x with SPI is equivalent to solving the optimization problem $Ax = b$ from the matrix of patterns $A = (a_{i,k})_{1<i<m,1<k<n}$ and the measurement vector $(b_i)_{1<i<m}$.

As variety of approaches corresponding to different choices of patterns exists to implement SPI. In a straightforward way, selecting an invertible matrix of patterns A provides an image reconstruction with a multiplication by A^{-1}. In that case, the number of measurements required equals the one of obtained pixels. Otherwise, optimization algorithms allows SPI with $m < n$. These approaches, qualified as *compressed sensing* allows to speed-up acquisitions while maintaining spatial resolution[7,8]. By analyzing the detector feedback during the acquisition, one can predict the more significant patterns and adopt an adaptive approach[9]. More recently, machine learning has proven its efficiency in retrieving the spatial information[10,11]. For reason of low numerical complexity, we follow a basis scan approach with shifted Hadamard matrix[12].

By comparison, to classical imaging, SPI allows the use of a detector with outstanding performance or lower price. For instance, it can perform in a spectral range where CCD are inefficient or with extra dimensions. As classical

photodetectors cannot capture more than two dimensions simultaneously, SPI opens the way for multidimensional imaging when applied to detectors owing extra dimension[12,13].

2.2 Experimental Set-up

To obtain the 4D dataset, we implement the SPI technique by coupling a DMD, a streak camera and a spectrometer as illustrated in Figure 3. The latter provides the measurements b_i in the form of images of the decay of the PL spectrum after a pulsed excitation with a temporal resolution of 35ps. The sample is excited with a pulsed TEM_{00} laser beam at 532nm transformed to a linear shape with appropriate optics. The photoluminescence is filtered and focused on the spatial light modulator (DMD). The modulated flux is collected through focusing optics and an optical fiber plugged into the spectrometer.

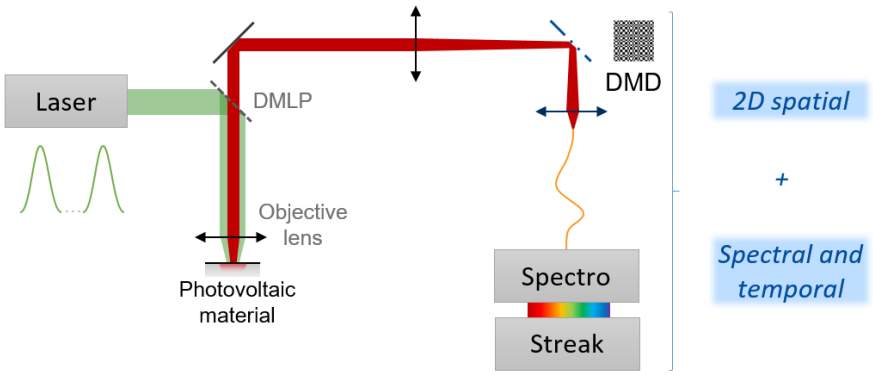

Figure 2: Schematic of the 4D-PL set-up

2.3 Optical management

The geometrical étendue of the detector of 0,0001 mm²/sr limits the collection of the 4D-PL set-up. In fact, the spectral and temporal resolutions are determined by the surface area of the light flux. A trade-off arises between these resolutions and the incoming light flux through the opening of the entrances slits. For sufficient resolutions, the input area is about 2500 µm² that induces a geometrical étendue comparable to the one of 25 pixels on a CCD. The fiber acts as a homogenizer and provides a field of view that does not depend on the slits aperture.

The choice of collection optics must take into account the stray diffraction of light induced by the DMD, which behaves like a 2D blazed grating[14]. Indeed, after reflection on the DMD, the light spreads according to an arc of roughly 21° in several diffraction orders. Collecting a small angle of refraction (as it would be the case with a single fiber) is equivalent to capturing a short bandwidth per order. Therefore, the optics need to collect a wide angle to transmit continuously the spectral range of interest.

2.4 Noise management

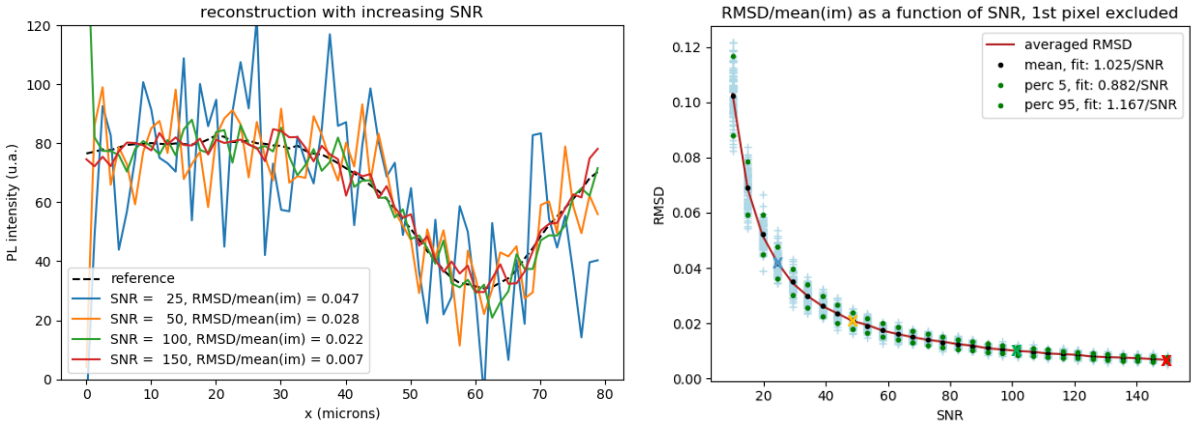

a. b.

Figure 3. a. Reconstruction by Single Pixel Imaging from a synthetic dataset for different signal to noise ratio; b. Dependence of the reconstruction quality (RMSD normalized by the averaged of the image) on the SNR.

As linear combination of streak acquisitions provide the local temporal evolution of the PL spectrum, the noises will sums up accordingly. As matter of fact, the Figure 3b-c illustrates the influence of the signal quality through examples of reconstructions with synthetic data. The simulated signal is calculated by introducing random noise to the reference measurements $\sum_{k=1}^{n} a_{i,k} * x_k$ where x_k is the reference pixel value and $a_{i,k}$ is the transmission of the projected pattern, either 1 or 0. A Gaussian distribution which variance is the averaged signal over the chosen signal to noise ratio (SNR) models the additional noise. Dark noise removal is taken into account by removing a noised signal of null average. In accordance with the experiments, the first pixel appears more sensitive to the noise and not taken into account of our analysis. Simulations of our approach show that the root mean square deviation of the spatially and temporally averaged intensity scales with the inverse of the signal to noise ratio. Therefore, it is crucial to ensure a minimum signal to noise ratio to ensure a satisfactory data reconstruction and the experiment must be designed accordingly. In that frame, the simulations can be used as references. They constitutes a tool to explore the implementation of different strategies to minimize the influence of noise as pattern splitting[15] or selection of patterns through semi nonnegative factorization technique[16]. As well, the efficiency of different families of patterns for our experiment dynamic can be investigated[17].

To enhance the signal to noise ratio, we have focused on 1D instead of 2D experiment at first. This makes the patterns identical along one direction which allows a higher signal intensity.

3. 4D ACQUISITION OF III-V WAFER

We demonstrate the 4D-PL set-up on 2 µm GaAs layer, sandwiched between 2 layers of GaInP 100 nm thick. The heterostructure was grown epitaxially by MOCVD on a GaAs wafer. We used~~s ata~~ high excitation to study a carriers dynamics after a short pulse. The samples are illuminated with the laser line generator at 500000suns at ambient temperature. We realize the single pixel imaging with 64 Hadamard patterns. Each measurement takes 10s resulting in a 10mn acquisition.

From the 4D recovered data is extracted the PL intensity profile at different times after the excitations shown in Figure 3a by integrating spectrally our 4D data. The approximated profile of the illumination is represented by the grey dashed In any pixel the temporal evolution of the spectrum can be obtained. An example is pictured in Figure 3b, where the decay during 1ns after the laser pulse and averaged from 67.6 to 75.2um is displaid. Moreover, it is possible to plot the normalized spectra to observe the peaks shift or broadening, as dislayed in Figure 3c for different locations on the sample. They all present a redshift that is highlighted by an exponential fit of the spectrum maximum (solid line). Furthermore, the dashed line figures the exponential fit at half maximum thresholds and emphasizes the spectrum narrowing during the decay.

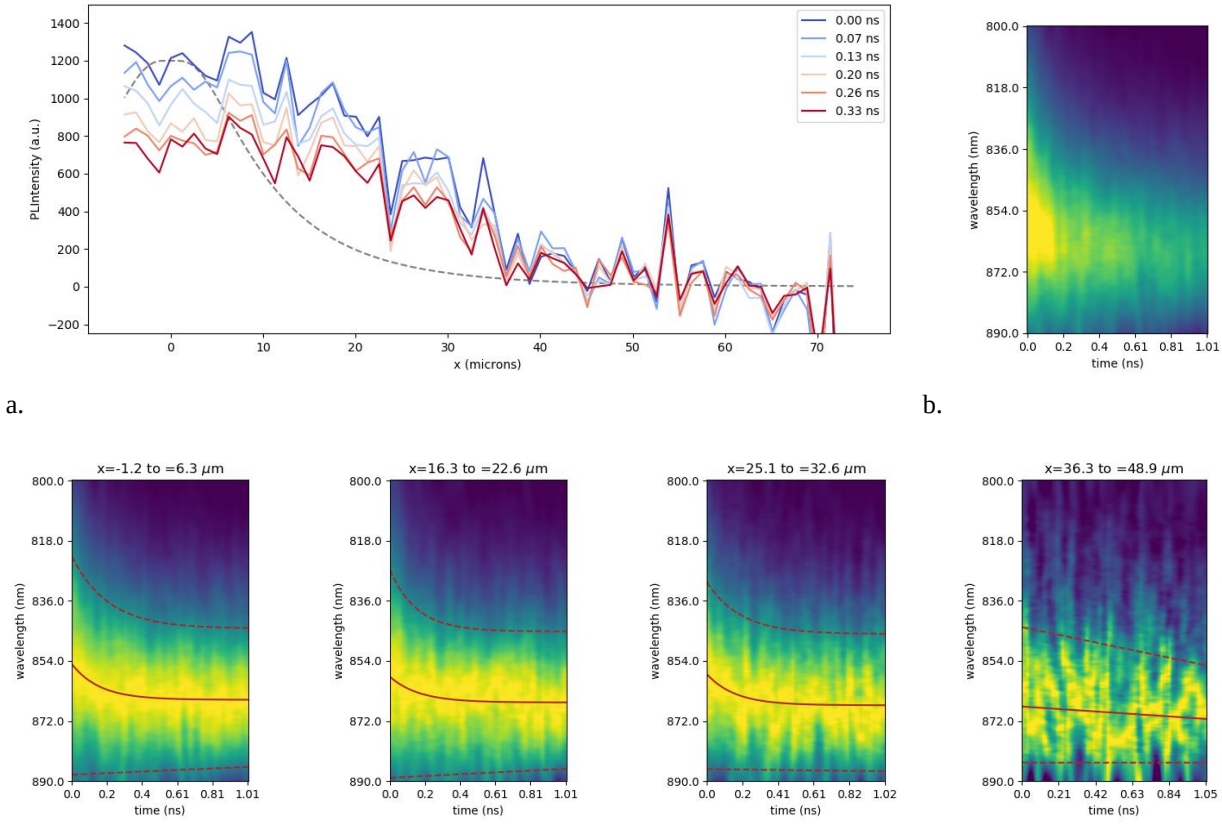

Figure 4: Examples of 4D acquisitions. a. PL profile at different time after the laser pulse (solid lines) and illumination profile (grey dashed line). b. Normalized PL decay averaged from -1.2 to 6.3µm resolved spectrally. c. PL spectra normalized at each time along the PL decay for different locations on the sample. The solid line features the spectral maximum, and the dashed line the thresholds at the half maximum.

Plots of figure 3 allow to extract spectral information, i.e. information on local energy distribution among carriers, evolving in space and time. This allows to track energy flows in the semiconductor after the initial pulse. For instance, the width of the PL emission, can be often related in a precise way to carrier temperature and spectral changes reveal carrier cooling[18].

4. CONCLUSION AND PERSPECTIVES

We have built a novel 4D photoluminescence imaging set-up that provides cartographies of the evolution of the photoluminescence spectrum after a pulsed excitation. We designed this instrument by implementing single pixel imaging. The choice of our experimental parameters is supported by numerical simulation to find a good trade-off between our constraints and the achieved resolutions (sub 100 ps time resolution, 10 µm spatial resolution). Our set-up allowed us to observe for the first time high energy slope variations and spectral shift at different distances from a focused excitation. Such information can help us investigating a wide range of phenomena owing a spectral signature. For instance, it can provide a new insight in the dynamic of hot carriers in the material or paves the way for a study of diffusion in the depth of the material.

REFERENCES

[1] Stolterfoht, M., Grischek, M., Caprioglio, P., Wolff, C. M., Gutierrez-Partida, E., Peña-Camargo, F., Rothhardt, D., Zhang, S., Raoufi, M., Wolansky, J., Abdi-Jalebi, M., Stranks, S. D., Albrecht, S., Kirchartz, T. and Neher, D., "How To Quantify the Efficiency Potential of Neat Perovskite Films: Perovskite Semiconductors with an Implied Efficiency Exceeding 28%," Adv. Mater. **32**(17), 2000080 (2020).

[2] Delamarre, A., "Characterization of solar cells using electroluminescence and photoluminescence hyperspectral images," J. Photon. Energy **2**(1), 027004 (2012).

[3] Bercegol, A., El-Hajje, G., Ory, D. and Lombez, L., "Determination of transport properties in optoelectronic devices by time-resolved fluorescence imaging," Journal of Applied Physics **122**(20), 203102 (2017).

[4] Yamada, T., Yamada, Y., Nakaike, Y., Wakamiya, A. and Kanemitsu, Y., "Photon Emission and Reabsorption Processes in CH 3 NH 3 PbBr 3 Single Crystals Revealed by Time-Resolved Two-Photon-Excitation Photoluminescence Microscopy," Phys. Rev. Applied **7**(1), 014001 (2017).

[5] Sridharan, A., Noel, N. K., Rand, B. P. and Kéna-Cohen, S., "Role of Photon Recycling and Band Filling in Halide Perovskite Photoluminescence under Focussed Excitation Conditions," J. Phys. Chem. C, acs.jpcc.0c09103 (2021).

[6] Bercegol, A., Ory, D., Suchet, D., Cacovich, S., Fournier, O., Rousset, J. and Lombez, L., "Quantitative optical assessment of photonic and electronic properties in halide perovskite," Nat Commun **10**(1), 1586 (2019).

[7] Duarte, M. F., Davenport, M. A., Takhar, D., Laska, J. N., Sun, T., Kelly, K. F. and Baraniuk, R. G., "Single-pixel imaging via compressive sampling," IEEE Signal Process. Mag. **25**(2), 83–91 (2008).

[8] Yu, W.-K., "Super sub-Nyquist single-pixel imaging by means of cake-cutting Hadamard basis sort," Sensors **19**(19), 4122 (2019).

[9] Rousset, F., Ducros, N., Farina, A., Valentini, G., D'Andrea, C. and Peyrin, F., "Adaptive Basis Scan by Wavelet Prediction for Single-Pixel Imaging," IEEE Trans. Comput. Imaging **3**(1), 36–46 (2017).

[10] Yao, R., Ochoa, M., Yan, P. and Intes, X., "Net-FLICS: fast quantitative wide-field fluorescence lifetime imaging with compressed sensing – a deep learning approach," Light Sci Appl **8**(1), 26 (2019).

[11] Higham, C. F., Murray-Smith, R., Padgett, M. J. and Edgar, M. P., "Deep learning for real-time single-pixel video," Sci Rep **8**(1), 2369 (2018).

[12] Rousset, F., "Single-pixel Imaging: development and applications of adaptive methods" (2017).

[13] Gattinger, P., Kilgus, J., Zorin, I., Langer, G., Nikzad-Langerodi, R., Rankl, C., Gröschl, M. and Brandstetter, M., "Broadband near-infrared hyperspectral single pixel imaging for chemical characterization," Opt. Express **27**(9), 12666 (2019).

[14] Rice, J. P., Neira, J. E., Kehoe, M. and Swanson, R., "DMD diffraction measurements to support design of projectors for test and evaluation of multispectral and hyperspectral imaging sensors," presented at SPIE MOEMS-MEMS: Micro- and Nanofabrication, 12 February 2009, San Jose, CA, 72100D.

[15] Pian, Q., Yao, R., Sinsuebphon, N. and Intes, X., "Compressive hyperspectral time-resolved wide-field fluorescence lifetime imaging," Nature Photon **11**(7), 411–414 (2017).

[16] Rousset, F., Peyrin, F. and Ducros, N., "A Semi Nonnegative Matrix Factorization Technique for Pattern Generalization in Single-Pixel Imaging," IEEE Trans. Comput. Imaging **4**(2), 284–294 (2018).

[17] Zhang, Z., Wang, X., Zheng, G. and Zhong, J., "Hadamard single-pixel imaging versus Fourier single-pixel imaging," Opt. Express **25**(16), 19619 (2017).

[18] Rosenwaks, Y., Hanna, M. C., Levi, D. H., Szmyd, D. M., Ahrenkiel, R. K. and Nozik, A. J., "Hot-carrier cooling in GaAs: Quantum wells versus bulk," Phys. Rev. B **48**(19), 14675–14678 (1993).